

# Feasibility of the LES for engineering problems

Toshio Kobayashi and Nobuyuki Taniguchi

*Institute of Industrial Science, University of Tokyo, Japan, and*

Shigenori Togashi

*Hitachi Ltd, Tsuchi-ura, Japan*

## Introduction

Turbulence is recognized as an essential phenomenon in heat transfer and fluid flow. Many attempts have been made to simulate the turbulence. Various turbulent models considering complex phenomena have been developed and successfully applied to engineering problems. It is, however, difficult still to predict the three-dimensional and unsteady effects in turbulence. On the other hand, although a direct simulation of turbulence gives us more accurate and precise data than experiments, it is essentially unsuitable for the high Reynolds number flows because of computational limitations.

A large eddy simulation (LES) seems a promising approach for the analysis of the high Reynolds number turbulence which contains three-dimensional and unsteady characteristics. Pioneering work on LES was carried out on the simulation of a simple channel flow by Deardorff[1], and more precise calculations by later works[2] confirmed its suitability for predicting turbulent flows. Although the LES was first applied to simple objects, it was also applied to complex flows in engineering processes. This research indicates that the LES enables an accurate prediction of turbulence, but spends much less CPU time than the direct simulation.

The basic idea of the LES is to calculate only larger than the grid size scale (called grid scale: GS) structures of turbulence, but to model smaller scale (called subgrid scale: SGS) structures. The governing equations for the GS quantities are derived by a spatial average or a filter procedure which removes SGS fluctuation from a Navier-Stokes equation. Because the smaller scale structures have more isotropic characteristics than larger scale ones, the model of SGS contribution can be simple but universal for various kinds of flow. Generally, a Smagorinski model based on an eddy viscosity concept has been used as an SGS model in previous works. For the incompressible flow, the equations of the GS quantities of velocity and pressure,  $\bar{u}$  and  $\bar{p}$  are expressed as,

$$\frac{\partial \bar{u}_i}{\partial x_i} = 0 \tag{1}$$

$$\frac{\partial \bar{u}_i}{\partial t} + \frac{\partial \bar{u}_i \bar{u}_j}{\partial x_j} = - \frac{\partial \bar{p}}{\partial x_i} + \frac{\partial}{\partial x_j} \left( \left( \frac{1}{\text{Re}} + \nu_i \right) \bar{S}_{ij} \right) \tag{2}$$

$$\nu_t = (Cs \Delta)^2 |\bar{S}|, \quad \bar{S}_{ij} = \frac{1}{2} \left( \frac{\partial \bar{u}_i}{\partial x_j} + \frac{\partial \bar{u}_j}{\partial x_i} \right), \quad \bar{S} = \sqrt{2S_{ij}S_{ij}} \quad (3)$$

where  $C_s$  is a constant coefficient of the Smagorinski model and  $\Delta$  is a characteristic length scale of the smallest GS structures which is practically defined by the grid size.

In order to apply the LES to engineering problems, the simulations need to be conducted in more complicated flow geometries and be under the various boundary conditions; thus some improvements of the SGS model are required. A boundary fitted grid which is connected with the finite difference method (FDM) or the finite element method (FEM) should be applied, too. They may bring some additional difficulties in the application of the SGS models and numerical methods.

In the following discussion, four examples of the LES will be presented to indicate the improvements to the SGS models and numerical methods for complicated engineering problems.

### Examples of LES for engineering problems

#### *Backward-facing step flow*

The flow over a backward-facing step displays typical features in complicated engineering problems, such as a flow separation, a reattachment and a recirculation, although its boundary geometry is still simple. In previous studies of the LES, a value of the model constant  $C_s$  depended on the types of flow and the grid resolution. Therefore it could not be adjusted easily for such a complex problem.

In this research, an improvement of the SGS model[3] was attempted. The formulation of the variable  $C_s$  originally developed by Yoshizawa[4] from a statistical analysis was,

$$\frac{C_s}{C_{s0}} = 1 + \frac{Ca}{S^2} \frac{DS}{Dt} \quad (0 \leq C_s \leq C_{s_{max}}) \quad (4)$$

New coefficients were optimized as  $C_{s0} = 0.10$ ,  $Ca = -32$  and  $C_{s_{max}} = -0.27$ , in both a decaying isotropic turbulence and a plane channel flow which corresponded to the highest ( $C_s = 0.23$ ) and the lowest ( $C_s = 0.1$ ) values recommended in the standard Smagorinsky model. The  $C_s$  calculated in this simulation was close to 0.1 in the main stream but about 20 per cent larger in the recirculating region.

A computational field had a backward-facing step whose expanding ratio was 1.5[5]. A fully developed channel flow was specified instantaneously at an inlet. For providing the inlet data, another LES of a channel flow was performed simultaneously. A cyclic condition was used in a spanwise direction. For the wall boundary, a practical approach[6] was adopted for the improvement of the prediction near the wall with a comparably coarse grid condition. A universal profile of mean velocity, known as a "law of wall"[7], gives,

$$F(y^+, u^+) = u^+ - y^+ + \exp(-\kappa \cdot B) \cdot \left[ \exp(\kappa \cdot u^+) - 1 - (\kappa \cdot u^+) - \frac{(\kappa \cdot u^+)^2}{2} - \frac{(\kappa \cdot u^+)^3}{6} \right] = 0 \quad (5)$$

Here,  $y^+$  and  $u^+$  are a distance from the wall and a velocity non-dimensionalized by a wall friction velocity. Supposing that an instantaneous velocity would fluctuate around the above profile, a velocity boundary condition was appropriately modelled even in the case that the nearest grid point from the wall was not in a viscous sub-layer.

An LES calculation using the above methods was performed by a grid of  $230 \times 50 \times 20$  points in the streamwise, channel width and spanwise directions respectively. The Reynolds number was 46,000 based on the inlet velocity and the step height. Figures 1 and 2 show profiles of mean velocity and turbulent intensity, comparing a present calculation using the LES and experimental data by Ito and Kasagi[8]. A good agreement was obtained even in the recirculating region, where most conventional models based on a Reynolds averaging gave poor prediction. The reattachment length was also predicted correctly as  $7.1H$ .

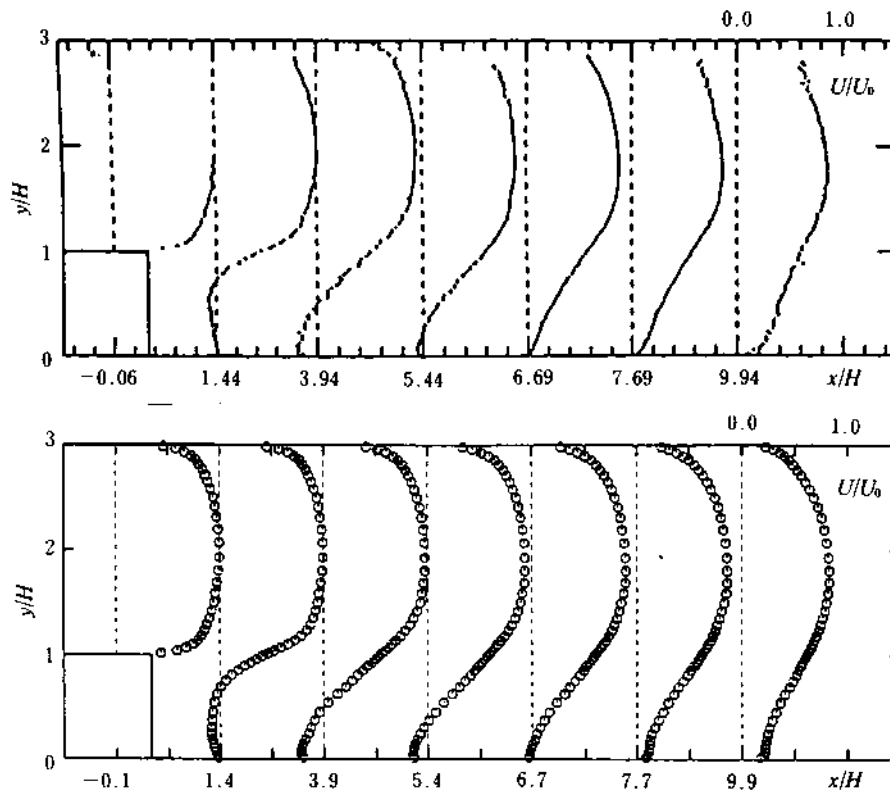


**Figure 1.** Mean streamwise velocity profiles of flow over a backward-facing step (above: experiment by Ito and Kasagi[8]; below: LES)

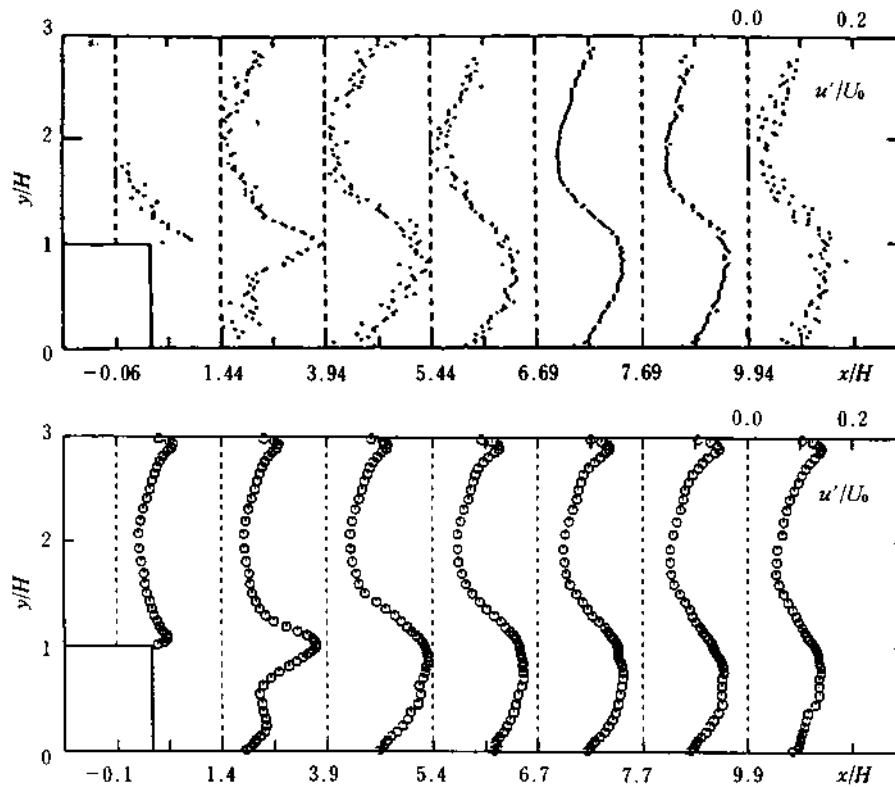


**Figure 2.**  
Streamwise turbulence  
intensity profiles of flow  
over a backward-facing  
step (above: experiment  
by Ito and Kasagi[8];  
below: LES)

### Plane jet

A turbulent jet flow is important in various industrial applications. Although the mean quantities have symmetric and simple profiles, the instantaneous fields are quite complicated. In spite of many experimental studies, further investigations will be necessary particularly on the dynamics of large coherent structures and laminar-turbulence transition, and the LES seems an appropriate approach to analyse them.

In the LES of the jet flow, an outlet boundary condition needs to be dealt with carefully so that numerical instability can be suppressed without serious numerical errors when vortexes flow out through the outlet boundary. From numerical investigations[9,10], it was recommended that the outflow velocity condition[10] should be based on a convection equation with a local effective convection velocity distribution on the outlet boundary. The expression was,

$$\frac{\partial \bar{u}}{\partial t} + U_{cA}(y) \frac{\partial \bar{u}}{\partial x} = C_3 \left\{ \frac{\partial}{\partial y} \left[ \left( \nu_t + \frac{1}{Re} \right) \left( \frac{\partial \bar{u}}{\partial y} + \frac{\partial \bar{v}}{\partial y} \right) \right] + \frac{\partial}{\partial z} \left[ \left( \nu_t + \frac{1}{Re} \right) \left( \frac{\partial \bar{u}}{\partial z} + \frac{\partial \bar{w}}{\partial x} \right) \right] \right\}$$

$$U_{cA}(y) = (C_1 U_{max} - U_A) \exp \left\{ - \left( \frac{y}{C_2 b_{ca}} \right)^3 \right\} + U_A \quad (6)$$

where a lateral component of viscous terms (right-hand side) was also added for stabilization. The local convection velocity,  $U_{cA}$  was modelled by a mean centre velocity,  $U_{max}$  and a half width of jet,  $b_{ex}$ , at the outlet boundary which could be calculated in the LES itself, and a small base velocity,  $U_A$  was set as 1 per cent of  $U_{max}$  in order to suppress numerical instability in the far side regions. Coefficients were optimized as  $C_1 = 0.8$ ,  $C_2 = 1.5$  and  $C_3 = 0.5$ .

In the MAC method used for an incompressible flow simulation, the pressure boundary condition should consist of the continuity equation for conserving a total mass balance. However, the condition derived from the normal component of momentum equation does not generally satisfy this consistency and may cause serious instability on the external boundary[11]. Therefore, the condition derived from the continuity equation was adopted in our simulations instead of the normal component of momentum equation generally used in previous LES research.

Using the above techniques, a plane turbulent jet was calculated for a Reynolds number of 6,000 based on the the nozzle width and velocity. The computational domain was in  $30D \times 40D \times 6D$  ( $D$ : nozzle width) and divided  $196 \times 146 \times 40$  grid points, to the streamwise (X), horizontal (Y) and spanwise (Z) directions respectively. The grid was expanded to the X- and Y-direction from the smallest grid size,  $0.1D \times 0.04D$  at the nozzle and the uniform grid as  $0.15D$  was used in the Z-direction. The third-order Runge-Kutta scheme was adopted in order to avoid a numerical disturbance from the time-marching discretization. The Smagorinski model was applied with the constant  $C_s = 0.12$ .

Mean velocity profiles at some different X positions are shown in Figure 3, where development of the velocity profile was reasonably predicted in upstream region ( $x < 7$ ). A predicted universal profile in the downstream region ( $x > 15$ ) was agreed with experimental data[12]. Development of turbulence intensity profiles shown in Figure 4 were predicted almost correctly in the middle ( $5 < x < 11$ ) and the downstream ( $x > 20$ ) regions. A universal profile was observed in the turbulent intensity as in the velocity. While there is a trend of overestimation of turbulent intensity, it would be dependent on the poor grid resolution at the core region ( $x < 3.5$ ) where small and coherent vortex structures were generated. A distribution of X component of vorticity is shown by a horizontal section view and three-dimensional isosurface in Figure 5. Around major vortexes, rib-like coherent structures were also observed in spanwise (Z) direction, which had not been indicated by the previous experimental works.

### LES on the boundary fitted grid system

#### *Circular pipe flow by the curvilinear co-ordinates*

The circular pipe may be the most commonly used element in fluid engineering. Although the polar co-ordinate system is naturally applied for dividing this figure into the computational grid, it has a singularity at the circular centre which causes a significant numerical problem. Therefore, a special procedure needs to be adopted in the LES calculations[13] with the polar co-ordinate.

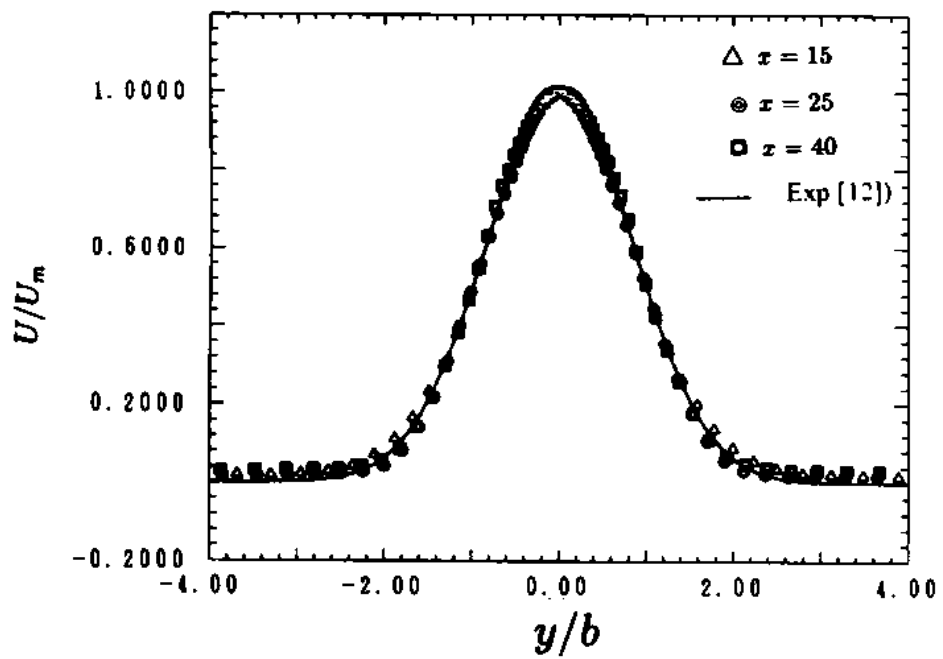
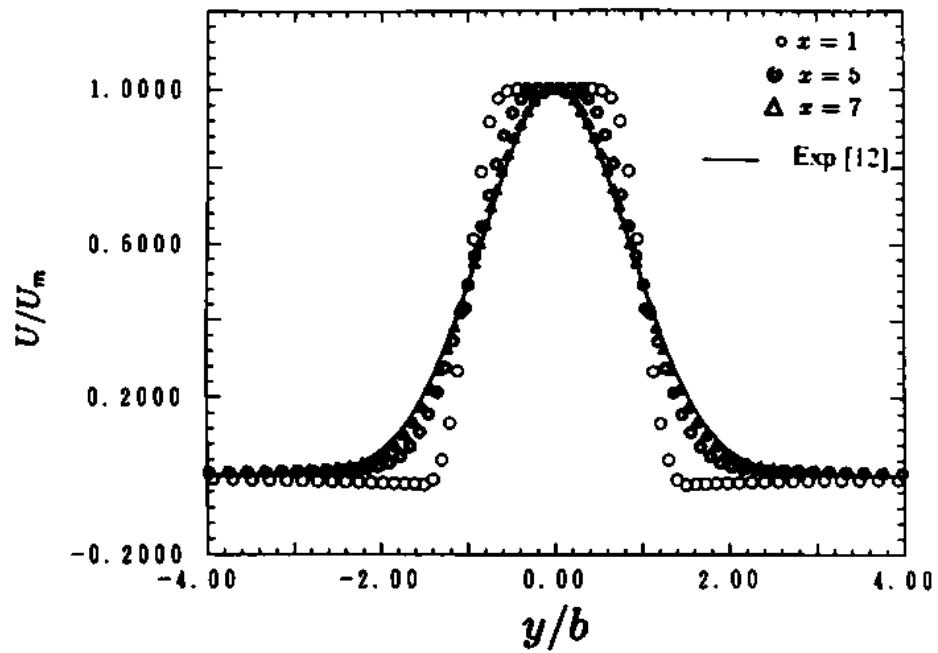


**Figure 3.**  
LES predicted profiles  
of streamwise velocity  
of a plane jet

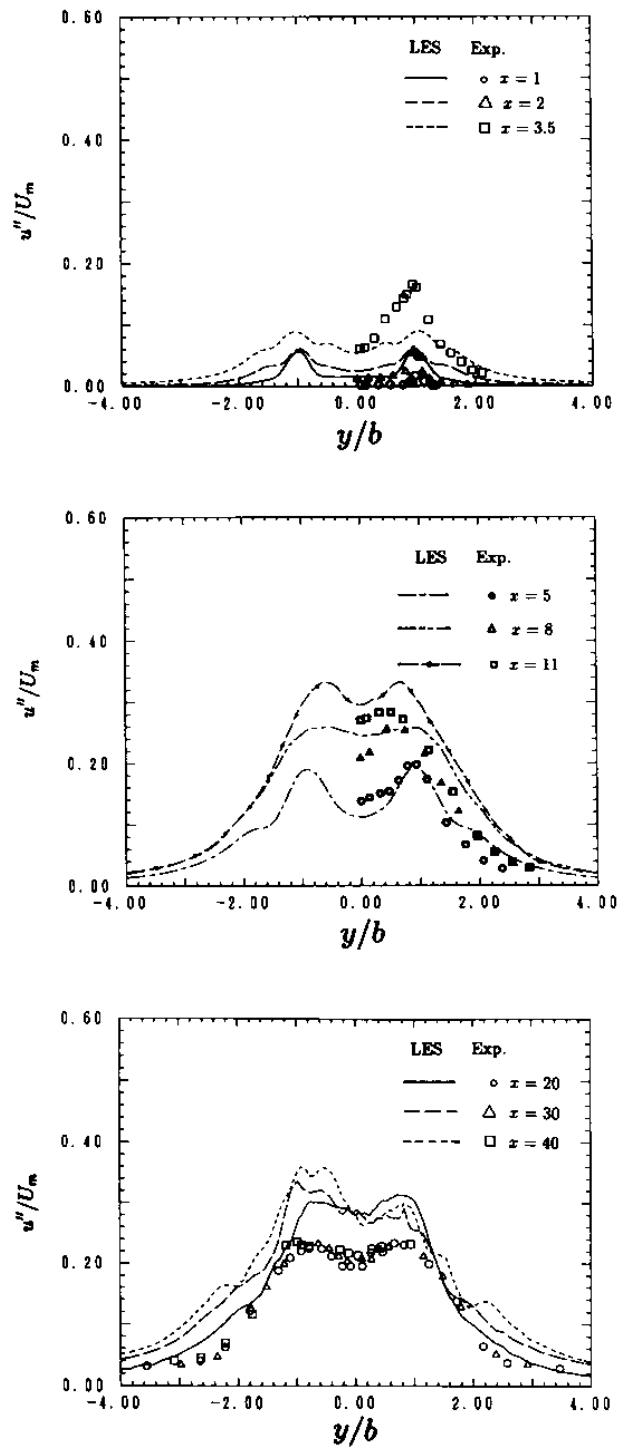


**Figure 4.**  
LES predicted profiles  
of streamwise  
turbulence intensity  
profiles

---

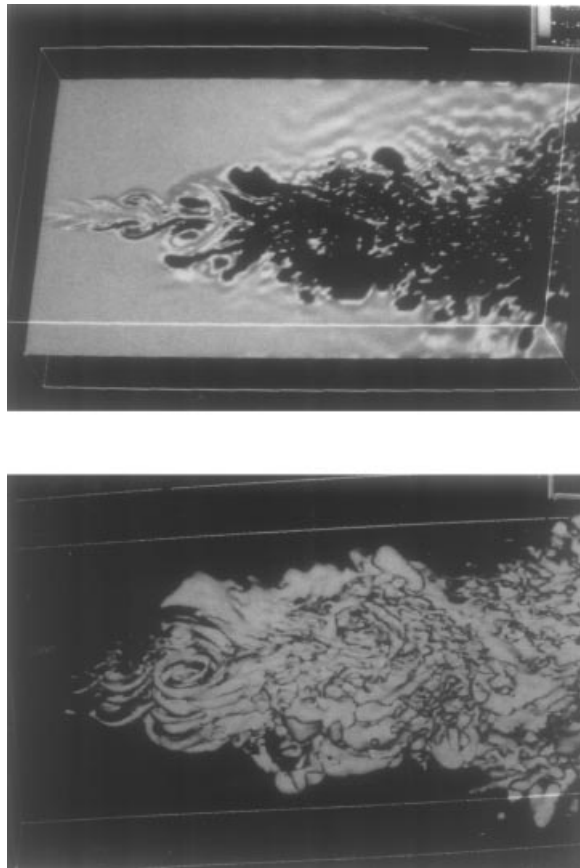


**Figure 5.**  
Distribution of  
streamwise vorticity  
component of a plane jet  
(above: horizontal  
section view; below: 3D  
isosurface)

---

While the general curvilinear co-ordinate seems a better solution considering the extension to other figures, it has a somewhat complicated formulation which needs more careful evaluation in respect of numerical errors.

In the research discussed below, a composite technique was introduced in order to reduce the numerical error; the general curvilinear and the polar co-ordinate grids shown in Figure 6 were used as an alternative for the time development equation and the calculation of the SGS model terms respectively. This method enabled a stable time-marching step on the curvilinear grid without central singularity, while the axisymmetry was correctly expressed in the SGS model calculation on the polar grid without the irregular numerical oscillations caused by the deformed grid.

A straight pipe flow was calculated at the Reynolds number of 420 based on the friction velocity (about 10,000 as that on the bulk velocity)[14]. The computational domain of  $R \times 2\pi \times 6.4R$  was discretized into  $40 \times 40 \times 80$  grid points. The minimum distance to the wall was  $y^+ = 2$  for the non-slip condition.



HFF  
7,2/3

A periodic boundary condition was imposed in the streamwise (Z) direction. The standard Smagorinski model was adopted. The model constant was  $C_s = 0.1$  and a damping function,

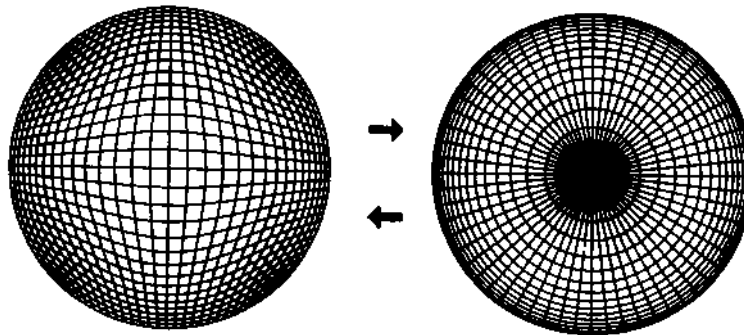
$$f(y^+) = 1 - \exp(-y^+/25) \quad (7)$$

was used near the wall as in the channel flow simulation

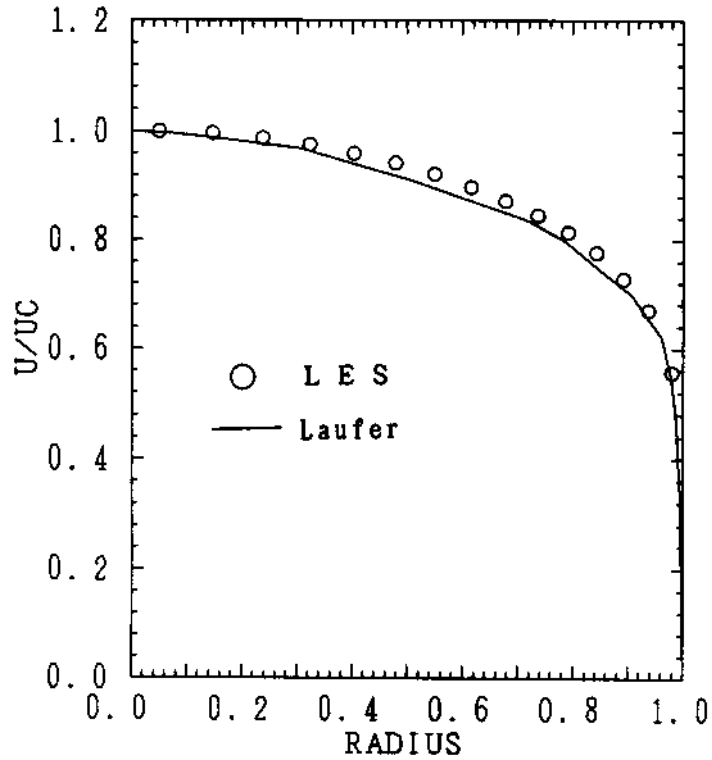
**244**

Numerical results of the LES were compared with the experimental data by Laufer[15]. A good agreement was obtained in the profiles of mean velocity and turbulence intensity as shown in Figures 7 and 8. Figure 9 shows the

**Figure 6.**  
Calculation grid for a circular pipe flow (left: curvilinear co-ordinate; right: polar co-ordinate)



**Figure 7.**  
Mean velocity profile in a circular pipe



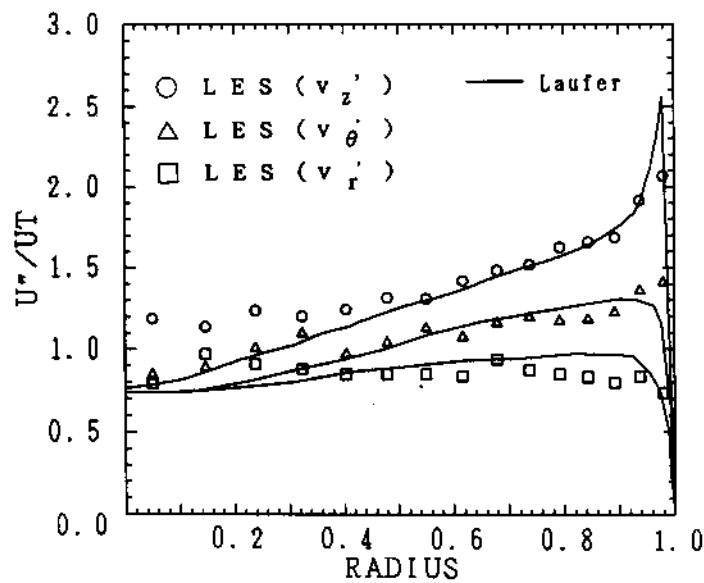


**Figure 8.**  
Turbulence intensity in  
a circular pipe

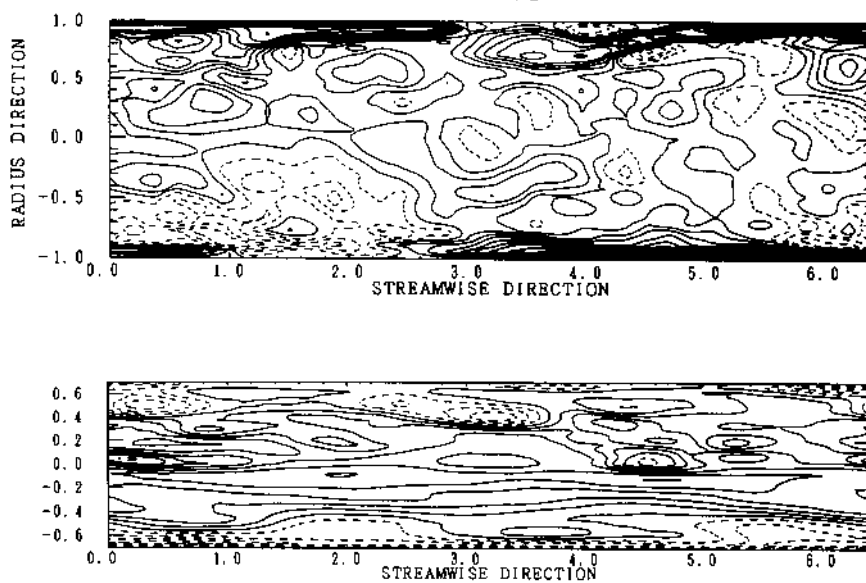


**Figure 9.**  
Instantaneous  
distribution of  
fluctuation streamwise  
velocity (above:  
meridional section;  
below: near wall  
surface)

instantaneous distribution of turbulent intensity in the meridional section and on the wall surface, where streak structures were recognized near the wall as in the channel flow. It also indicated that the composite grid technique effectively avoided the problems by the singularity lines and the strong grid deformation.

#### *Channel flow LES by FEM*

For the simulation of complicated geometry, the finite element method (FEM) formulated on the unstructured grid has more feasibility than the finite

difference method (FDM) generally used for the previous LES. Although the FEM has been adapted to various kinds of flow simulation, there are few applications for LES[16]. So this research was first done for the optimization of the Smagorinski constant  $C_s$  on the FEM formulation because it was reported that the  $C_s$  depended on grid resolution in the FDM simulation. The object was a channel flow with periodic condition, well known as a standard problem for the LES validation. It was confirmed that the most recommended value in the FDM simulation,  $C_s = 0.1$ , should be also adaptable to the present FEM mentioned below.

Governing equations were transformed into residual equations by a weighted residual method and discretized spatially by the Galerkin method, where the same basis functions both for the variables and the weight function. A concentrating mass method was adopted for the effective calculation of the mass matrix from the volume integration[17]. A hexahedral bilinear element shown in Figure 10 was adopted. For the time integration scheme, a MAC method with a slight modification for the FEM formulation[18] and the second-order Adams-Bashforth scheme was applied.

These FEM techniques were used commonly in the high Reynolds number flow simulation, but there was a practical problem in that the FEM tended to require a larger calculation time than the FDM. From experience, in a typical calculation about 42 per cent of total CPU time was required to calculate the convection term when it was discretized by the accurate Galerkin formulation. In order to reduce the CPU time, the following modification,

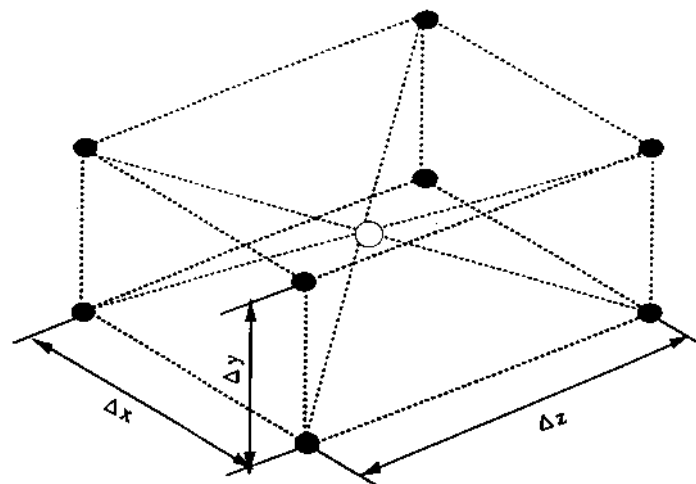


**Figure 10.**  
Conceptual view of an  
FEM element

(● :velocity nodes, ○ :pressure node)

$$\bar{u} \frac{\partial \bar{u}_i}{\partial x_j} = \bar{U} \frac{\partial \bar{u}_i}{\partial x_j} \quad (8)$$

was adopted for the matrix calculation of convection term, where the capital letter  $U$  denotes the element mean velocity defined as a representative value in each element. As a result, the CPU time for the calculation of convection matrix was reduced to only 1 per cent of the total CPU time which would have a comparable efficiency to that of the FDM.

The analysis model was a plane channel flow; the computational domain of  $3.2H \times H \times 1.6H$  ( $H$ : channel width) was divided into the 40,960 elements which were equivalent to the  $32 \times 40 \times 32$  points of the FDM grid. The elements were clustered to the wall direction (Y) and the minimum size was  $y^+ = 3$ . Periodic conditions were applied to the streamwise (X) and the spanwise (Z) direction. A non-slip condition was used on the wall. The standard Smagorinski model was applied and the constant  $C_s$  was optimized as 0.1.

The calculation results[19] are shown in Figure 11 by mean velocity profile, turbulence intensity and turbulence shear stress, where all the data were non-dimensionalized by a wall friction velocity. A universal velocity profile in viscous and logarithmic layers indicated by dashed lines was well predicted and turbulence shear stress predicted by the GS fluctuation  $\langle u'v' \rangle$  traced well on the theoretical line. Three components of turbulent intensity were correlated with the experiment by Kreplin and Eckerman[20] and the direct simulation by Kim *et al.*[21] as well as the FDM simulation using the same grid resolution.

### Discussions and future directions

The four examples of the LES presented in this paper were attempted for the application of LES to engineering problems. Acceptable results could be obtained by using some modifications in the Smagorinski SGS model and the numerical methods. They would demonstrate the feasibility of LES for predicting the various turbulent flows.

While it has been reported that a few recently developed SGS models[22,23] have better adaptability than the previous Smagorinski model for the flows under the extra force by gravity or rotation and for the transition phenomena from laminar to turbulence, they also seem to provide good alternatives for the practical simulations when their numerical problems are solved.

Additionally, the computer utilities used for the present work and typical CPU times are listed in Table I. All calculations were performed by original programs developed for high performance computers with array processors. The CPU time was not exact but typical for each program. It is still not easy to apply the LES to engineering problems owing to large computation costs. However, the newest supercomputers with multi-CPU architecture have more than ten times the performance of those used for this study and their memory capacity is large enough to deal with complicated grid systems. Parallel

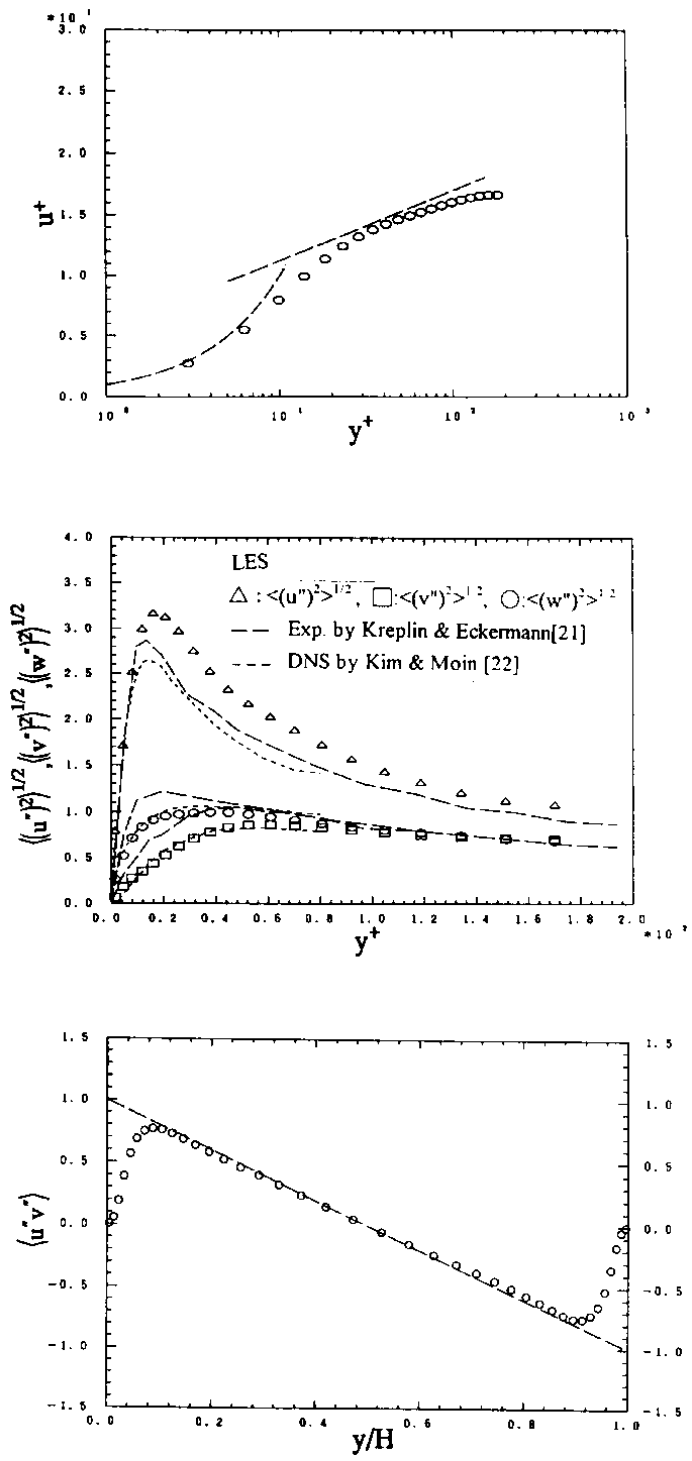


**Figure 11.**  
Prediction by the LES  
using FEM formulation  
(top: mean velocity  
profile; middle:  
turbulence intensity;  
bottom: turbulence  
shear stress)

computing and adaptive grid techniques will have to be adopted effectively so as to combat the difficulties of using such new computer architecture.

LES for  
engineering  
problems

| Case                    | No. of grid points<br>(or elements) | Time steps total<br>(for averaging) | CPT time<br>(hours) | Computer type<br>(peak performance) |
|-------------------------|-------------------------------------|-------------------------------------|---------------------|-------------------------------------|
| Backward-facing<br>step | 230 × 50 × 20                       | 20,000 (6,000)                      | 100                 | Fujitsu VP100 (250MFlops)           |
| Plane jet               | 196 × 146 × 40                      | 16,000 (4,000)                      | 50                  | Fujitsu VP2600 (5GFlops)            |
| Circular pipe by<br>BFC | 40 × 40 × 80                        | 40,000 (10,000)                     | 35                  | Fujitsu VP100 (250MFlops)           |
| Channel flow by<br>FEM  | 40,960 elements                     | 50,000 (10,000)                     | 20                  | Hitachi S3800 (3GFlops)             |

249

**Table I.**  
Computer utilities and  
CPU time

#### References

1. Deardorff, J.W., *J. Fluid Mech.*, Vol. 41 Pt 2, 1970, pp. 453-81.
2. Moin, P. and Kim, J., *J. Fluid Mech.*, Vol. 118, 1982, pp. 341-77.
3. Morinishi, Y. and Kobayashi, T., *J. of JSME B*, Vol. 57 No. 540, 1991, pp. 2602-5 (in Japanese).
4. Yoshizawa, A., *Phys. Fluids*, Vol. A3 No. 8, 1991, pp. 2007-9.
5. Morinishi, Y. and Kobayashi, T., *Engineering Turbulence Modelling and Measurements*, Elsevier Applied Science, Barking, Essex, 1990.
6. Morinishi, Y. and Kobayashi, T., *J. of JSME B*, Vol. 57 No. 540, 1991, pp. 2595-601 (in Japanese).
7. Spalding, D.B., "Trans. ASME", *J. Appl. Mech.*, Vol. 28, 1961, pp. 455-8.
8. Ito, J. and Kasagi, N., *Nagareno Kasika*, Vol. 9 No. 4, 1989, pp. 245-8 (in Japanese).
9. Dai, Y., Kobayashi, T. and Taniguchi, N., *Int. J. of JSME*, Series B, 1994, Vol. 37 No. 2, pp. 242-53.
10. Dai, Y. and Kobayashi, T., *JSME 69 Tuujousoukai*, Vol. B, 1992, pp. 311-13 (in Japanese).
11. Dai, Y. and Kobayashi, T., *Month. J. of Institute of Industrial Science*, University of Tokyo, Vol. 46 No. 2, 1994, pp.135-8 (in Japanese).
12. Thomas, F.O. and Goldschmidt, V.W., *J. Fluid Mech.*, Vol. 163, 1986, pp. 227ff.
13. Eggels, J.G.M. and Nieuwstadt, F.T.M., "Large eddy simulation of turbulent flow in an axially rotating pipe", Ninth Symposium on Turbulent Shear Flows, 1993, pp. 310.1-310.4.
14. Togashi, S. and Kobayashi, T., The 3rd JSME-KSME Fluid Eng. Conference, 1994.
15. Laufer, S., *NACA Report*, No. 1174, 1954.
16. Kato, C. and Ikegawa, M., *ASME FED-117*, 1991, pp. 49-56.
17. Kawahara, M., *Finite Element Analysis of Fluid Dynamics*, Nikkagiren Publisher, Tokyo, Japan, 1985 (in Japanese).
18. Oshima, M., PhD thesis, University of Tokyo, 1991.
19. Kobayashi, T., Tsubokura, M., Oshima, M. and Taniguchi, N., The 3rd JSME-KSME Fluid Eng. Conference, 1994.
20. Kreplin, H. and Eckermann, M., *Phys. Fluids*, Vol. 22, 1979, pp. 1233-9.
21. Kim, J., Moin, P. and Moser, R., *J. Fluid Mech.*, Vol. 177, 1987, pp. 133-66.
22. Horiuti, K., *Phys Fluids*, Vol. A5, 1993, pp.146ff.
23. Moin, P. and Jimenez, J., *AIAA paper No. 3099*, 1993.